



## Radiographic and Computed Tomographic Anatomy of the Fetlock, Pastern and Coffin joints of the Manus of the Donkey (*Equus asinus*)

Mohamed E. Amin, Raafat M.A. Elbakary, Mohamed A.M. Alsafy, Naglaa Fathi

Anatomy and Embryology Department, Faculty of Veterinary Medicine, Alexandria University

### Key words

Donkey, CT, Radiology, Cast, Gross anatomy

### Abstract:

The digit of the donkey as a draught animal is commonly susceptible to much affection. The purpose of the present study was to provide a detailed anatomic reference of radiographic and computed tomographic images in conjunction with cross and sagittal sections of the normal fetlock, pastern and coffin joints of the donkey for anatomists, surgeons and veterinary students. Eight adult donkeys of both sexes free from any joints affection were used in our study. The digit of two donkeys had undergone radiographic and computed tomographic scanning; the other donkey's specimens were used to anatomical dissection and sectional anatomy. In the computed tomography (CT) of the fetlock joint all bone structures of the joint appeared also the soft tissue structures that could be identified and evaluated on the different soft tissue window planes included the common digital extensor tendon, lateral digital extensor tendon, superficial digital flexor tendon (SDFT), deep digital flexor tendon (DDFT), straight, oblique, and cruciate distal sesamoidean and intersesamoidean ligaments. For the pastern joint the structures that can be identified including the proximal phalanx, DDFT and digital cushion. In the coffin joint the collateral sesamoidean ligament (CSL) is difficult to identify on CT images.

Corresponding Author: Mohamed Alsafy, [safy73@yahoo.com](mailto:safy73@yahoo.com)

### 1. Introduction

The donkey is an important farming animal used heavily by the Egyptian farmers because of their great tolerance as a draught animal. Computed tomography examinations have become more common in veterinary medicine due to the availability of the computed tomography machine in teaching institutions and private veterinary hospitals (Pollard and Puchalski, 2011). The using of the new anatomical techniques in studying anatomy as the radiology, computed tomography and others techniques being useful for both student and anatomist as well as surgeon. Imaging techniques play a major meanwhile a few CT studies on horse's foot have been role in the modern biomedical research (Olsen et al., 2007) and (Olsen and Winterdahl, 2009). CT, through its high spatial resolution and moderate differentiation of tissue contrast is a fastened exceptionally useful technique for visualizing general anatomy (Dixon and Dacre, 2005). Accurate interpretation of ultrasonography or CT of the foot requires a thorough knowledge of the cross sectional anatomy of the region and accurate

interpretation of the plan metric CT is necessary for the study and evaluation of the pathological condition or damaged tissues (Raji et al., 2008) and (Weissengruber et al., 2006). CT is particularly useful for looking at complex bony structures such as the skull, spine or joints. The involvement of the new techniques (Digital X-ray images, computed tomography, magnetic resonance imaging, ultrasonography, endoscopy, fluoroscopy, 3D Image, animation, CDs) in the anatomy tutorial in Egypt, as well as in the other Arabic countries becomes essential to follow the international steps and to prepare the students to the clinical stage of veterinary study (Saber, 2008). CT was efficient imaging modality that provides a cross-sectional image with superior soft tissue differentiation and no superimposition of the overlying structures, which can be used for better diagnosis of foot and foot pad abnormalities (Badawy, 2011). Radiography remains the main stay of equine musculoskeletal imaging due to its low cost, ready accessibility and global evaluation of bony structures (Kinns and Nelson, 2010). The using of the normal radiographic anatomy,

computed tomographic scans, cross and sagittal sections and the gross anatomical dissection of the digit is very important for anatomists, surgeons and veterinary students to the accurate investigations of the fetlock, pastern and coffin joints of the donkey. So the current study is focused on the anatomical details of these joints.

## 2. Material and methods

Eight adult donkeys of both sexes free from any joints affection were used in our study.

### Gross anatomy

Eight fore limbs of donkey used for studying the gross anatomy of the fetlock, pastern and coffin joints. The donkeys are being bled after being anesthetized then undergone routine preservative technique (10% formalin mixed with 4% glycerin and 1% phenol for 10-15 days until complete fixation and then the fore limbs were separated and the three joints dissected for studying the gross anatomy. Three of these donkeys fore limb were injected using gum milk latex with paint in the joint cavity of fetlock, pastern and coffin joints then preserved in freezer for three days then dissected for studying the joint capsule of each joint and its pouches if present.

### Computed tomography

Two fore limbs of donkey were used for studying CT of the three joints. The donkey was being anesthetized then being bled and the three joints were severed and transferred to the CT center within 24 hours and imaged using a Toshiba asteion super 4 multi slice 4 CT apparatus. The distance between the slices taken was 0.5 cm.

### Radiology

Two fore limbs of donkey were obtained after the donkey being anesthetized and being bled and transferred to the x-ray center within two hours and imaged using Toshiba 500ml apparatus for x-rays in dorsopalmar view.

### Cross and sagittal sections

Four donkeys' fore limbs were obtained after the donkey being anesthetized and being bled well then the digits was cut using electric band saw with 0.5 cm slices interval. The slices were preserved in freezer for 24 hrs and being imaged using a digital camera, matched with the correlated CT images.

## 3. Results

### Fetlock joint

#### Gross anatomy

The **Articular surfaces** of the fetlock joint are the head of the metacarpus, proximal extremity of the 1<sup>st</sup> phalanx (Fig.1). The head of the large metacarpal bone consists of two condyles separated by a sagittal ridge; the medial condyle is the largest (Fig.1/B). The proximal extremity of the proximal phalanx is consists of two articular cavities for articulation with the two condyles of the large metacarpal bone (Fig.1/A). The medial cavity is slightly larger than the lateral one. The two proximal sesamoid bones have the shape of three sided pyramids, their dorsal surface articulates with the condyles of the large metacarpal bone (Fig.1/C). Each of the proximal sesamoid bones carries a sagittally elongated articular facet for articulation with the palmar part of the crossponding condyle on the distal extremity of the large metacarpal bone.

The **joint capsule** is capacious and attached around the articular surfaces. It consists of fibrous and synovial layer. The fibrous layer is distinct on the dorsal aspect of the joint. It is somewhat thick and on the side it is closely adhered to the collateral ligaments from which it cannot be identified as an independent structure. On the palmar surface the fibrous capsule is difficult to distinguish and it is represented by the synovial layer only. There is a bursa which interposed between the tendons of common digital extensor muscle dorsally and the fibrous capsule of the fetlock joint palmarly. The synovial layer forms two pouches, dorsal and palmar pouch. The dorsal pouch is cone shape with the base directed distally (Fig.2/B). It extends for about 2 cm on the 3<sup>rd</sup> metacarpal bone. The palmar pouch is thin walled lies between the distal extremity of 3<sup>rd</sup> metacarpal bone and the suspensory ligament to the point of its bifurcation (Fig.2/A). It is covered by the suspensory ligament, superficial and deep digital flexor tendons. This pouch forms a proximal palmar pouch under suspensory ligament and a distal palmar pouch.

#### Ligaments

The ligaments can be classified into collateral and sesamoidean ligaments. The **collateral ligaments** are medial and lateral collateral ligaments. They are divided into two layers, superficial layer which arises from the eminence on the side of the distal end of the 3<sup>rd</sup> metacarpal bone and passes to the rough area distal to the margin of the articular surface of the proximal phalanx; the deep layer is

shorter and stronger. It arises from the depression on the side of the distal end of the 3<sup>rd</sup> metacarpal bone and passes obliquely distally and palmarly and inserted on the abaxial surface of the proximal sesamoid bone and the proximal end of the 1<sup>st</sup> phalanx. The **suspensory ligament**; the fibers of the suspensory ligament or M. Interosseus is attached proximally to the palmar aspect of distal row of carpal bones, the palmar carpal ligament and the proximal part of the palmar surface of the large metacarpal bone. They coalesce to form a strong musculotendinous band that runs down in the metacarpal groove between two splint bones on the palmar surface of the large metacarpal bone. At the distal fourth of the metacarpus it divides into two diverging branches. Each branch passes to the abaxial surface of the corresponding sesamoid bone. Then it passes obliquely distally and dorsally to the dorsal surface of the proximal phalanx to attach with the common digital extensor tendon (extensor branch). There is a bursa between extensor branch and the proximal end of the 1<sup>st</sup> phalanx. The **lateral and medial collateral sesamoidean ligaments** connect the proximal sesamoid bones to the metacarpus proximally and to the 1<sup>st</sup> phalanx distally. The **straight sesamoidean ligament** is a strong band of fibers originates proximal to the sesamoid bones and inserts on the palmar border of the base of the 1<sup>st</sup> phalanx. The **oblique sesamoidean ligament** was represented by strong bands. It is narrow proximally and wide distally passes from the base of the proximal sesamoid bones and the adjacent part of the intersesamoidean ligament to the proximal 4<sup>th</sup> of the palmar surface of the proximal phalanx. The **cruciate sesamoidean ligament** includes two bands crucially disposed across the distopalmar aspect of the fetlock joint. The fibers of each band are attached proximally to the base of the respective sesamoid bone and adjacent part of the intersesamoidean ligament. They extend obliquely towards the opposite palmar tubercle on the base of the 1<sup>st</sup> phalanx. The **intersesamoidean ligament** is represented by a narrow dense fibrocartilaginous mass filling the interval between the adjacent proximal sesamoid bones. Proximally, this mass extends beyond the sesamoid bones for about 0.5 cm and thus provides an additional surface for articulation with the ridge on the head of the large metacarpal

bone. The **short sesamoidean ligament** is strong but short. They extends from the base of the sesamoid bone close to its articular surface and passes distally between the joint capsule of the fetlock joint dorsally and the distal sesamoidean ligament palmarly to be attached on the palmar border of the base of the 1<sup>st</sup> phalanx close to the articulation with the corresponding sesamoid bone.

#### **Computed tomography**

Three precontrast CT images were selected (Fig.3) and matched with their corresponding anatomic sections: in a transverse plane and 2 in a sagittal plane (Fig.4). All bone structures, including the diaphysis of MCIII, the condyles and the sagittal ridge of MCIII, the proximal sesamoid bones and the proximal phalanx were seen on transverse and sagittal images. All images had excellent delineation between the cortex and medulla of the bones. The soft tissue structures that could be identified and evaluated on the different soft tissue window planes included the common digital extensor tendon, lateral digital extensor tendon, SDFT, DDFT; straight, oblique, and cruciate distal sesamoidean ligaments and intersesamoidean ligament. The collateral sesamoidean ligaments and the short distal sesamoidean ligaments could be seen but not always clearly identified. The metacarpointersesamoidean ligament could not be identified. The common and lateral digital extensor tendons were oval shaped on the transverse images and clearly seen. The flattened SDFT (on transverse images) was smoothly margined and its margins were clearly demarcated on the transverse and sagittal reconstructions. The straight distal sesamoidean ligament originates from the base of the proximal sesamoid bones and the intersesamoidean ligament and inserts distally on the second phalanx where it forms with the SDFT the scutum medium. Proximally, the straight distal sesamoidean ligament had a trapezoidal shape; in the middle, a rectangular to square shapes; and distally, became oval. The oblique distal sesamoidean ligaments had a heterogeneous appearance. In the middle of the proximal phalanx the obliquedistal sesamoidean ligaments appeared as small triangular structures deep to the straight distal sesamoidean ligament adjacent to the bony surface of the proximal phalanx. The cruciate distal sesamoidean ligaments were best evaluated

on the transverse plane. On the sagittal reconstructions, the differentiation between the cruciate, oblique, and straight distal sesamoidean ligaments could not be made at the origin site on the base of the proximal sesamoid bones. The short distal sesamoidean ligaments extend from the dorsal aspect of the base of the proximal sesamoid bones to the palmar margin of the articular surface of the proximal phalanx. The short distal sesamoidean ligaments were quite difficult to identify, resulting from the difficulty to differentiate them from the oblique sesamoidean ligaments. The separation between the short and oblique distal sesamoidean ligaments was best seen on the transverse images, although it was difficult to discern. The short distal sesamoidean ligaments were not recognizable as separate from the oblique sesamoidean ligaments in the sagittal planes. The metacarpointersesamoidean ligament originates on the palmar distal aspect of MCIII and fuses with the intersesamoidean ligament. This ligament could not be identified.

#### **Pastern joint**

##### **Gross anatomy**

The *articular surfaces* of the pastern joint consist of the distal extremity of the proximal phalanx and the proximal extremity of the middle phalanx (Fig.5). The articular surface on the distal extremity of the proximal phalanx is composed of a shallow sagittal groove separating two condyles. The medial condyle is slightly larger, and the two are separated by a notch (Fig.5/B). The proximal extremity of the middle phalanx (Fig.5/A) consists of two articular cavities separated by a low ridge for articulation with the distal extremity of the proximal phalanx. The two articular cavities are oval in outlines and are equal in width. On the dorsal border there is an elevation which forms extensor process.

The *joint capsule* blended with the common digital extensor tendon dorsally, the collateral ligaments medially and laterally and the straight sesamoidean ligament palmarly. On the dorsal surface of the joint the fibrous layer of the joint capsule is thick and is intimately blended with the fascia of the region. On the sides the fibrous layer is adherent to the collateral ligaments from which it cannot be separated as an independent structure. On the palmar surface the fibrous layer cannot be identified. The synovial layer forms two pouches,

dorsal and proximal palmar pouch. The dorsal pouch is extends for about 1.5cm on the dorsal aspect of the shaft of the proximal phalanx. It is covered somewhat by the common digital extensor tendon. The proximal palmar pouch extends along the distal 4<sup>th</sup> of the palmar aspect of the proximal phalanx. Its free convex borders have a foston like appearance (Fig.6).

##### **Ligaments**

The ligaments of the pastern joint are collateral and palmar ligaments. The *Medial and lateral collateral ligament* arise from a depression surrounded by a tubercle on the corresponding aspect of the proximal phalanx and gain attachment to an eminence on the corresponding aspect on the base of the middle phalanx. The *Palmar ligaments* consist of four ligaments which are central pair and medial and lateral ligaments. The medial and lateral ligaments attached proximally to the middle of the border of the 1<sup>st</sup> phalanx while the central pair attached more distally and on the margin of the rough triangular area of the 1<sup>st</sup> phalanx.

##### **Computed tomography**

In CT images of the pastern joint of donkey the structures that can be identified including the proximal phalanx, DDFT and digital cushion (Fig.7).

#### **Coffin joint**

##### **Gross anatomy**

The *articular surfaces* of the coffin joint include the distal extremity of the middle phalanx, the proximal extremity of the distal phalanx and distal sesamoid bone (Fig.8). The distal extremity of the middle phalanx consists of two articular condyles separated by a sagittal groove. The two articular condyles encroach on the dorsal surface and more on the palmar surface (Fig.8/A). The articular surface of the distal phalanx consists of two articular cavities separated by a sagittal low ridge. The two cavities are oval in shape and are concave dorsally and convex palmarly (Fig.8/B). The articular surface tapers dorsally to form extensor process. The distal sesamoid bone consists of two articular facets separated by a vertical ridge (Fig.8/C). These facets are facing proximally and dorsally. Its dorsal articular surface contacts the distal end of PII; a narrow distal facet touches PIII.

The *joint capsule* is attached around the margin of the articular surfaces of the bones entering in the

formation of the coffin joint. It is reinforced on either side by the collateral ligaments of the joint. Dorsally; the capsule is supported by the tendon of the common digital extensor muscle while palmarly the tendon of the deep digital flexor muscle provides the necessary support. On distension, the joint capsule forms two pouches, dorsal and palmar. The dorsal pouch is located undercover of the terminal part of the tendon of insertion of the common digital extensor muscle. On the other hand, the palmar pouch is larger than the dorsal one and extends along the distal 3<sup>rd</sup> of the palmar surface of the middle phalanx. Palmarly, the pouch is related to the collateral sesamoidean ligament distally and the tendon of the deep digital flexor muscle proximally.

#### **Ligaments**

The ligaments of the coffin joint include the collateral ligaments and the ligaments of the distal sesamoid bone. The *medial and lateral collateral ligaments* are short and strong bands attached proximally in a depression on either side of the distal part of the 2<sup>nd</sup> phalanx and distally end on the depression on either side of the extensor process. The **ligaments of the distal sesamoid bone**; the *distal sesamoidean impar ligament* extends from the distal border of the distal sesamoid bone to the palmar border of the 3<sup>rd</sup> phalanx. The *Collateral sesamoidean ligaments* were attached proximal to the depressions on each side of the distal end of the 1<sup>st</sup> phalanx and ends on the proximal border of the distal sesamoid bone but give a branch to the axial surface of each cartilage and angle of the 3<sup>rd</sup> phalanx.

#### **Computed tomography**

Two precontrast CT images were selected and matched with their corresponding anatomic sections (Fig.9). All bone structures including the 2<sup>nd</sup> phalanx, 3<sup>rd</sup> phalanx, condyles of 2<sup>nd</sup> phalanx, articular cavities of 3<sup>rd</sup> phalanx and distal sesamoid bone were seen on transverse and sagittal images. All images have excellent delineation between the cortex and medulla of the bones. The DDFT and digital cushion were identified. The sagittal images show the complete distal extremity of 2<sup>nd</sup> phalanx and proximal extremity of 3<sup>rd</sup> phalanx. The distal interphalangeal collateral ligaments is difficult to be identified especially near their distal attachment to the distal phalanx. the CSL is difficult to identify on CT images.

#### **Radiology of the fetlock, pastern and coffin joints**

On dorsopalmar radiographs (Fig.10), the fetlock joint is approximately symmetrical about the prominent sagittal ridge of the distalmetacarpus, although the medial condyle is slightly wider than the lateral. The sagittal ridge articulates with a groove in the proximal phalanx. The joint space is approximately at right angles to the long axis of the third metacarpal bone. The middle phalanx is approximately half the length of the proximal phalanx. There are two prominent bony ridges on either side of the distal aspect of the bone, where the collateral ligaments of the coffin joint originate. The articular surface of the distal end of the middle phalanx normally has a smooth curved outline, which extends dorsally into a point. The central third of the articular surface may be relatively flatter than the more dorsal and palmar aspects. The articular surfaces of the proximal and middle phalanges in the pastern joint are otherwise reasonably congruous. The navicular bone is largely obscured by the extensor process of the distal phalanx.

#### **4. Discussion**

The present investigation was carried out to characterize the anatomic features of the fetlock, pastern and coffin joints of the donkey by use of gross anatomy, CT and radiology.

The general morphological features of the articular surfaces entering in the formation of the fetlock joint of the donkey show great resemblance to these of the horse (Getty, 1975; Dyce et al., 2010). Concerning the joint capsule of fetlock joint, it is observed that the joint capsule forming a dorsal pouch and palmar pouch, a similar result was also reported by Getty (1975) and Skerritt and McLelland (1984) in horse. In the donkey the palmar pouch have two parts a proximal and distal palmar pouch. The ligaments of the fetlock joint of the donkey are similar to that observed in horse (Getty, 1975; Dyce et al., 2010).

Results of the study indicated that not only the bony structures but also the clinically important soft tissue structures could be well identified by use of CT. Computed tomography has proven its usefulness in the diagnosis of subchondral bonecysts (Rijkenhuizen et al. 2005), osteomyelitis of the axial border of the proximal sesamoid bones (Barbee et al. 1987, Hanson et al.

1996, Rijkenhuizen et al. 2005) and condylar fractures (Morgan et al.2006).

Computed tomography is an excellent imaging modality for evaluation of bony structures. In the present study, CT provided excellent discrimination between the cortex and medulla of MCIII, the proximal sesamoid bones, and the proximal phalanx. Differentiation between the superficial and deep parts of the collateral ligaments of the fetlock joint could not be made. Because of their attachment sites, separation at those sites was a possibility. This is in agreement with results of CT of the carpus (Kaser-Hotz, 1994). Differentiation between the cruciate, oblique, and straight distal sesamoidean ligaments and between the short and oblique sesamoidean ligaments at their origin site on the proximal sesamoid bones could not be made on the sagittal reconstructions as well as differentiation between the sagittal part of the oblique distal sesamoidean ligament and straight distal sesamoidean ligament on the transverse planes and between the collateral sesamoidean ligaments and superficial part of the collateral ligaments. Differentiation between the short and oblique distal sesamoidean ligaments on the transverse images was difficult. Separation of the structures with the same density, such as the short, cruciate, oblique, and straight sesamoidean ligaments, the superficial and deep part of the collateral ligaments and the collateral sesamoidean ligaments with the superficial part of the collateral ligaments, remains difficult with CT (Tucker et al., 2001). Computed tomography allowed a full assessment of the fetlock joint because of the good soft tissue and bone images that were obtained at the same time. Therefore, knowledge of the normal anatomy is essential, and results of the present study could be used as a basis for evaluation of CT images of the limbs of donkeys with fetlock joint injuries.

The results obtained on the articular surfaces and the capsule of the pastern joint of the donkey are essentially similar to those recorded on the corresponding articulation of the horse (Getty, 1975), (Skerritt and Mcllland, 1984) and (Dyce et al., 2010).

Dissection has revealed that in donkey, as in horse (Getty, 1975) and (Dyce et al., 2010) the pastern joint is provided with collateral and palmar ligaments. The collateral ligaments of the joint in

the donkey have a similar character to those reported by (Getty, 1975) in the horse.

Concerning the palmar ligaments, the present findings have revealed that they represented by two branches (axial and abaxial) which are attached proximally to a rough area about the middle of the corresponding border of the 1<sup>st</sup> phalanx to the complementary fibrocartilage of the 2<sup>nd</sup> phalanx. These findings agreed with (Dyce et al., 2010) in horse.

Concerning the CT of the pastern joint of the donkey, computed tomography scan is excellent imaging modality. Its usage in veterinary medicine is, however, limited as it is expensive and the animal should be anaesthetized (Raji et al., 2008 and Garland et al., 2002). Nevertheless, it has some potential advantages over the routine radiography; it provides across-sectional image with superior soft tissue differentiation and no superimposition of the overlying structures, which can be used for better diagnosis of abnormalities and for evaluating the extent and severity of the lesion (Walker et al., 1993).

On CT images the joints and the digital blood vessels were represented the exact radiolucent (hypodense) structures having the least density, these might be attributed to their contents are fluids (Raji et al., 2008 and Jain and Gupta 2004). The articular surfaces and the capsule of the coffin joint in donkey show a close similarity to that of the horse (Getty, 1975 and (Dyce et al., 2010).

The synovial membrane forms dorsal and palmar pouches in the present work as well as in the horse. Getty (1975) observed that the coffin joint of ox has three pouches a considerable pouch behind and on each side small pouches projecting against the cartilage of the 3<sup>rd</sup> phalanx. In camel the only pouch which was observed by Morcos (1955) is the dorsal one. Concerning the number and attachments of the ligaments of the coffin joint in donkey are similar in general to that mentioned by Getty (1975) and Dyce et al (2010) in horse.

Concerning CT of the coffin joint advances in diagnostic techniques are continuously sought to assist clinical practitioners of veterinary medicine with making a definitive diagnosis, providing an accurate prognosis and determining the most appropriate treatment strategy. In the present study the CT images of the donkey coffin joint

provides acceptable details of the anatomical structures and were correlated well with its corresponding gross anatomical specimens. In accordance with some authors (Barbee et al., 1987, Peterson & Bowman, 1988, Dick, 1995) in horse, in bovine (Raji et al., 2008.) and in small ruminant (Bahgat, 2007), in dog (Fike et al., 1981, 1984). The CT provides good discrimination between bone and soft tissue architectures.

Thus the computed tomography (CT) has become an important diagnostic imaging modality in the diagnosis of the musculoskeletal disorders (Bienert & Stadler, 2006). The coffin joint comprised of the distal phalanges, the navicular bone, the impar ligament and the collateral sesamoidean ligament (CSL). Normally, the peri-articular and subchondral bone surfaces are smooth and well delineated. The cartilage of the joint is relatively thick but not identified on CT unless a CT arthrogram is performed (Puchalski et al., 2005) in horse. In the present study the coffin joint of donkey in CT sections and cross anatomical sections appeared bounded palmarly by digital cushion. This is similar to that observed by (El-shafy and Sayed-Ahmed, 2012) in one-humped camel and Egyptian water buffalo.

The condyles of the MCIII or MTIII bone and sesamoid bones should be superimposed on each other and the MCP/MTP joint space should be identifiable (Park, 2000).

### 5. Conclusion

The knowledge of the advanced techniques as CT and radiograph of the fetlock, pastern and coffin joints of the donkey beside the normal anatomy help in treatment of several injuries occurring in these joints. Also these techniques help students in learning and studying the anatomy of these joints with more details and easily.

### 6. References

Badawy, M. 2011. Computed Tomographic Anatomy of the Fore Foot in One-Humped Camel. *Global Veterinaria* 6 (4): 417-423.

Bahgat, H. 2007. Computed Tomography and Cross Sectional Anatomy of the Metacarpus and Digits of the Small Ruminants. *Benha Vet. Med. J.*, 18:63-84.

Bienert, A., Stadler, P. 2006. Computed tomographic examination of the locomotor apparatus of horses a review. *Pferdeheilk* 22:218-26.

Barbee, D.D., Allen, J.R., Grant, B.D. 1987. Detection by computed tomography of occult osteochondral defects in the fetlock of a horse. *Equine Vet J*.19:556-558.

Dyce, K.M., Sack, W.O., Wensing, C.J.G. 2010: Text book Of Veterinary Anatomy, 4<sup>th</sup> Ed. Saunders.

Dixon, P.M., Dacre, I. 2005. A review of equine dental disorders. *Veterinary J.*, 169(2): 165-187.

Dick, K. J. 1995. Computed tomography of the head of horses. *Magyar Allatorvosok Lapja*, 50:309-11.

El-shafy, A., Sayed-Ahmed, A. 2012. Computed tomography and cross sectional anatomy of the metacarpus and digits of the one-humped camel and Egyptian water buffalo. *Int. J. Morphol.* 30(2):473-482.

Fike, J. R., LeCouteur, R. A., Cann, C. E. 1984. Anatomy of the canine orbital region. *Vet. Radiol. Ultrasound*, 25:32-6.

Fike, J. R., LeCouteur, R. A., Cann, C. E. 1981. Anatomy of the canine brain using high resolution computed tomography. *Vet. Radiol. Ultrasound*, 22:236-43.

Garland, M.R., Lawler, L.P., Whitaker, B.R., Walker, I.D.F., Corl, F.M. and Fishman, E.K. 2002. Modern CT applications in veterinary medicine. *Radiographics*, 22(1): 399-415.

Getty, R., 1975: Sission and Grossmans the Anatomy of Domestic Animals, 5<sup>th</sup> Ed, vol.1. Philadelphia, PA: W.B. Saunders.

Hanson, J.A., Seeherman, H.J., Kirker-Head, C.A. 1996. The role of computed tomography in evaluation of subchondral osseous lesions in seven horses with chronic synovitis. *Equine Vet J.* 28:480-488.

Jain, R.K., Gupta, A.N. 2004. Arterial supply of the fetlock, pastern and coffin joints of fore limb in camel (*Camelus Dromedarius*). *Haryana Veterinarian*, 43: 15-18.

Kinns, J., Nelson, N. 2010: Imaging tarsal trauma. *Equine Vet. Edu.* 22, 296-298.

Kaser-Hotz, B., Sartoretti-Schefer, S., Weiss, R. 1994. Computed tomography and magnetic resonance imaging of the normal equine carpus. *Vet Radiol Ultrasound*. 35:457-461.

Morgan, J.W., Santschi, E.M., Zekas, L.J. 2006. Comparison of radiography and computed tomography to evaluate metacarpal/metatarsophalangeal joint pathology of paired limbs of thoroughbred racehorses with severe condylar fracture. *Vet Surg.* 35:611-617.

Morcos, W. M. 1955. *Bovine Anatomy*. 1<sup>st</sup>, Ed. Burgess, Minneapolis.

Olsen, A.K. and Winterdahl, M. 2009. Imaging techniques in large animals. *Scandinavian J. Laboratory Animal Sci.*, 36(1): 55-66.

Olsen, A.K., Zeidler, D., Pedersen, K., Sorensen, M., Jensen, S.B., Munk, O.L. 2007. Imaging techniques: CT, MRI and Pet scanning, pp 387-395. In *Swindle MM: Swine in laboratory. Surgery, anesthesia, imaging and experimental techniques*. CRC press.

Pollard, R, Puchalski, S. 2011. CT contrast media and applications. In: Schwarz T and Saunders J, (Eds.): Veterinary Computed Tomography. Wiley-Blackwell, 2011:57-65.

Puchalski, S. M., Snyder, J.R., Hornof, W.J., Macdonald, M.H., Galuppo, L.D. 2005. Contrast enhanced computed tomography of the equine distal extremity . In: 51 Annual Convention of the AAEP, ivis.org, Seattle, WA, USA.

Park, R.D. 2000. Optimal radiographic views for evaluating thoroughbred yearlings - quality control of the radiographic image. In: 46th Annual Convention of the American Association of Equine Practitioners. San Antonio, Texas, USA. Pp: 357-358.

Peterson, P. R., Bowman, K .F. 1988. Computed tomographic anatomy of the distal extremity of the horse. *Vet. Radiol. Ultrasound*, 29:147-56.

Raji, A.R., Sardari, K., Mohammadi, H.R. 2008. Normal cross-sectional anatomy of the bovine digit: comparison of computed tomography and limb anatomy. *AnatomiaHistologiaEmbryologia, Journal of Veterinary Medicine. C.*, 37: 188-191.

Rijkenhuizen, A.B.M., van den Top, G.B., van den Belt, A.J. 2005. The role of computed tomography in the surgical management of cystic lesions. *Pferdeheilk.* 21:317-321.

Saber, A.S. 2008. Implementing Imaging Facilities and Multimedia in Teaching Veterinary Anatomy. *J. vet. anat.* Vol 1 No1: 48-53.

Skerritt, G.C., McLelland, J. 1984. *Functional Anatomy of the Domestic Animals.* John Wright and Sons Ltd.

Tucker, R.L., Sande, R.D. 2001. Computed tomography and magnetic resonance imaging of equine musculoskeletal conditions. *VetClin North Am EquinePract.* 17:145-157.

Walker, M., S. Hartsfield, N. Matthews, G. White, M. Slater and J. Thoos, 1993. Computed tomography and blood gas analysis of anesthetized bloodhounds with induced pneumothorax. *Veterinary Radiology and Ultrasound*, 34: 93-98.

Weissengruber, G.E., Egger, G.F., Hutchinson, J.R., Groewold, H.B., Elsasser, L., Famini, D. and Forstenpointner, G. 2006. The structure of the cushions in the feet of African elephants (*Loxodonta Africana*), *J. Anatomy.* 209: 781-792.

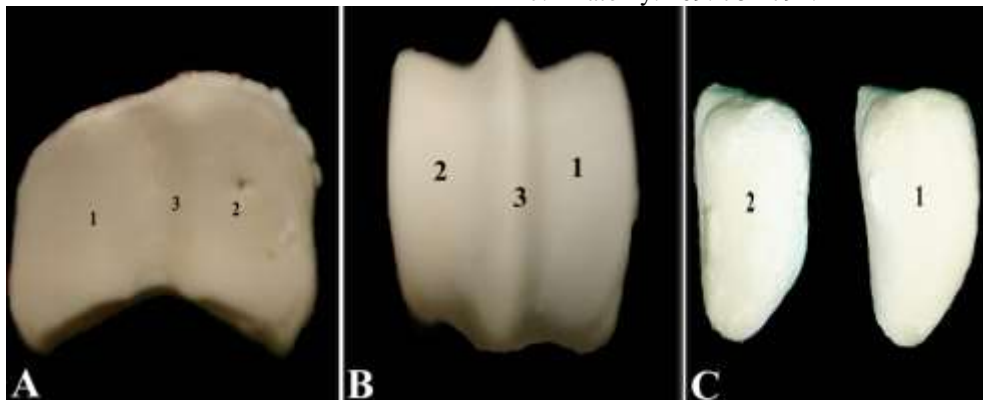


**Figure (1)** bones of fetlock joint of donkey. Image A: proximal extremity of 1<sup>st</sup> phalanx. 1= medial condyle. 2= lateral condyle. 3= sagittal ridge. B: distal extremity of MCIII. 1=lateral articular surface. 2= medial articular surface. 3= sagittal groove. C: 1, 2= proximal sesamoid bones.

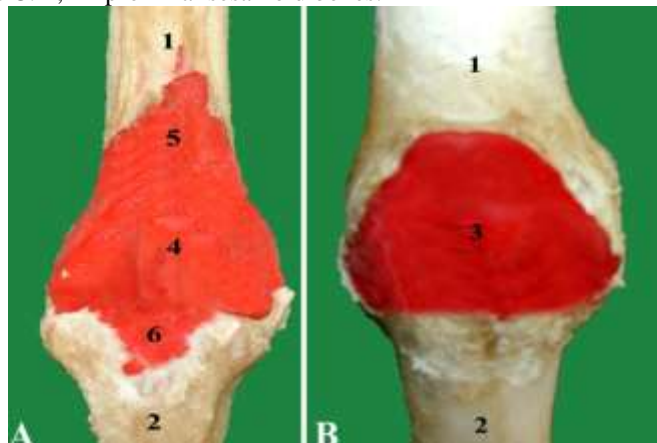


**Figure (2)** fetlock joint injected with colored latex showing the joint capsule of the joint and its pouches. A= image of palmar pouch. B= image of dorsal pouch. 1= MCIII. 2= 1<sup>st</sup> phalanx. 3= dorsal pouch. 4= palmar pouch. 5= proximal palmar pouch. 6= distal palmar pouch.

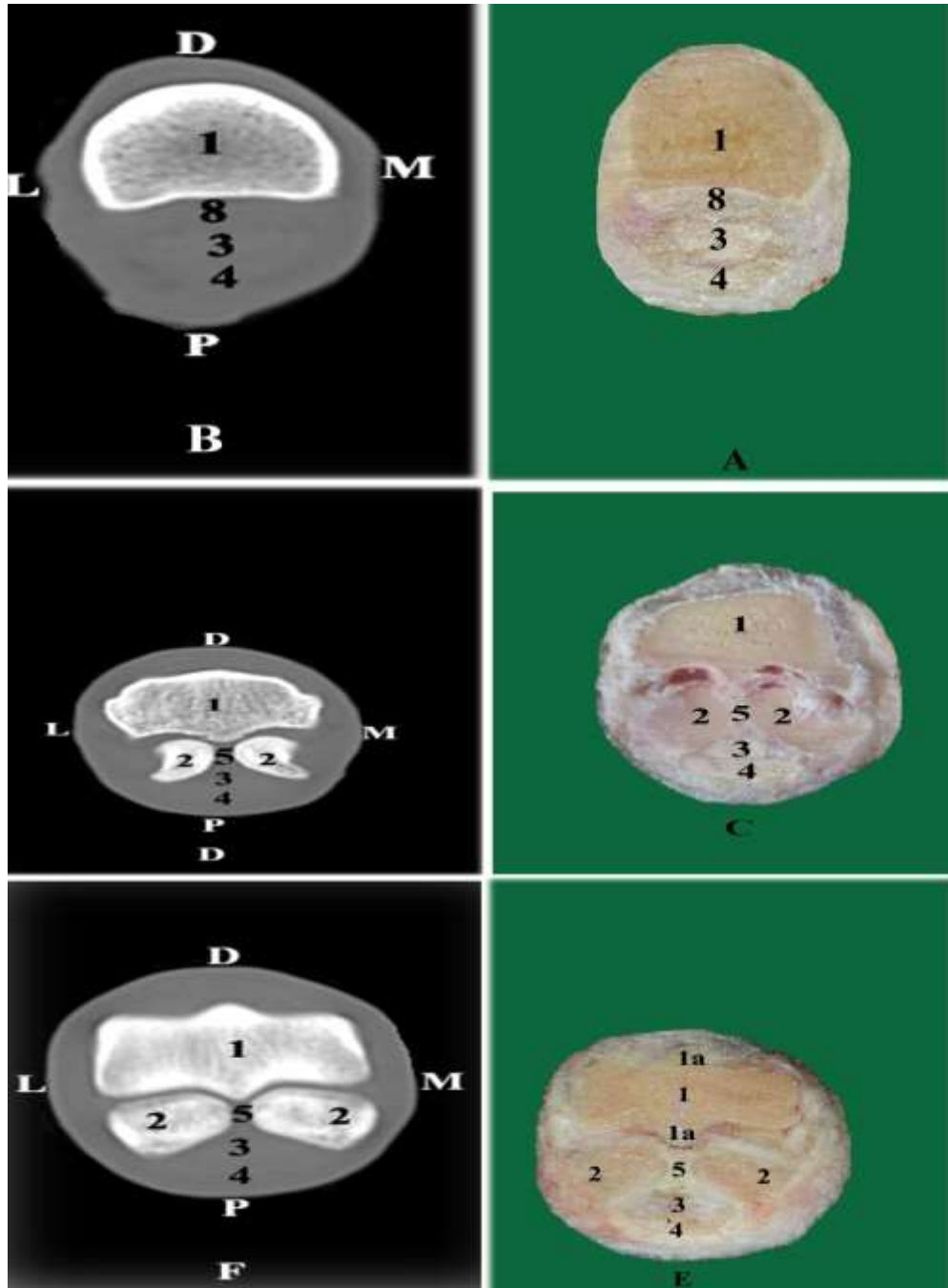


**Figure (3)** photograph of transverse anatomic section (right) and transverse CT views (left) of normal fetlock joint in donkey sequentially displayed from proximal to distal. 1=MCIII. 1a= sagittal ridge of MCIII. 2= proximal sesamoid bone. 3=DDFT. 4= SDFT. 5= intersesamoidean ligament. 6= suspensory ligament.

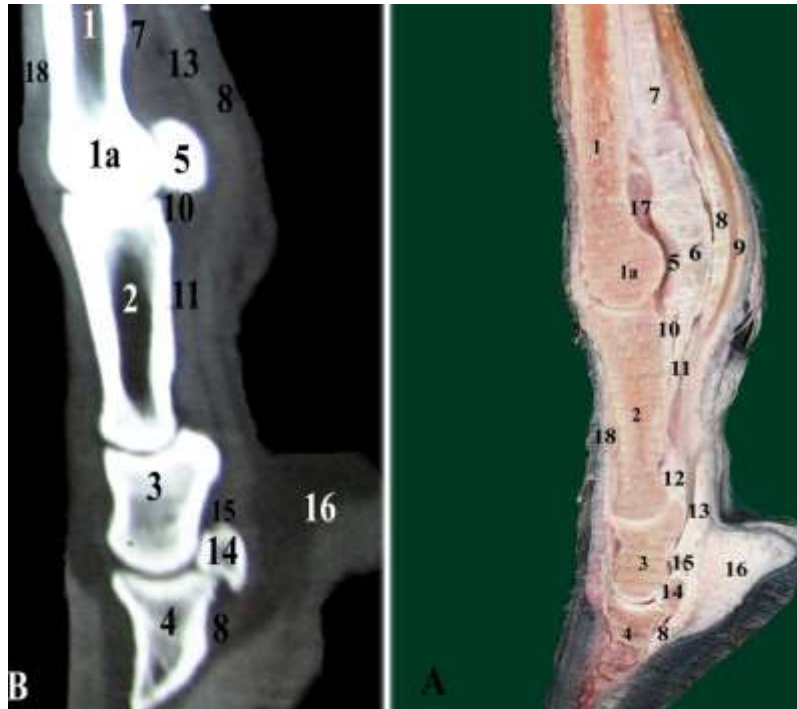


**Figure (4)** photographs of the sagittal anatomic section (B) and sagittal reconstructed CT image of the normal fetlock joint (A). 1= MCIII. 1a= distal extremity of MCIII. 2= 1<sup>st</sup> phalanx. 3= 2<sup>nd</sup> phalanx. 4=3<sup>rd</sup> phalanx. 5=proximal sesamoid bone. 6= intersesamoidean ligament. 7= suspensory ligament. 8= DDFT. 9= palmar annular ligament. 10=oblique sesamoidean ligament. 11= straight sesamoidean ligament of distal sesamoid bone. 12=middle scutum. 13= SDFT. 14= distal sesamoid bone. 15= collateral sesamoidean ligament of the distal sesamoid bone. 16= digital cushion. 17= proximal palmar pouch of MCP joint. 18= dorsal digital extensor tendon.

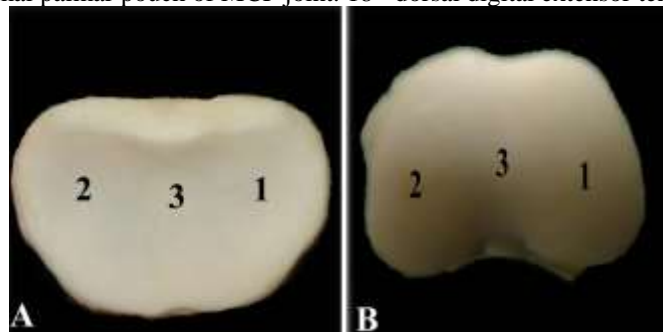


**Figure (5)** photograph of the articular surfaces of the pastern joint of the donkey. B= distal extremity of the 1<sup>st</sup> phalanx. 1=medial condyle. 2=lateral condyle. 3= sagittal groove. A= proximal extremity of 2<sup>nd</sup> phalanx. 1= lateral articular cavity. 2= medial articular cavity. 3=sagittal ridge.



**Figure (6)** photograph of the pastern joint injected with latex showing joint capsule. 1= palmar pouch. 2= proximal palmar pouch. 3= 1<sup>st</sup> phalanx. 4= middle scutum.

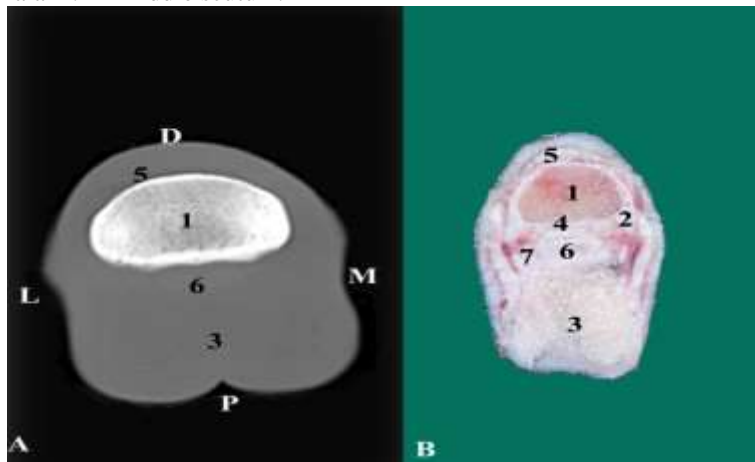


**Figure (7)** CT image (A) of the pastern joint matched with its corresponding anatomic section (B). 1= 2<sup>nd</sup> phalanx. 2=collateral ligament of the PIP joint. 3= digital cushion. 4=fibrocartilaginous surface of PIP joint. 5= dorsal digital extensor tendon. 6= DDFT. 7= distal digital annular ligament.

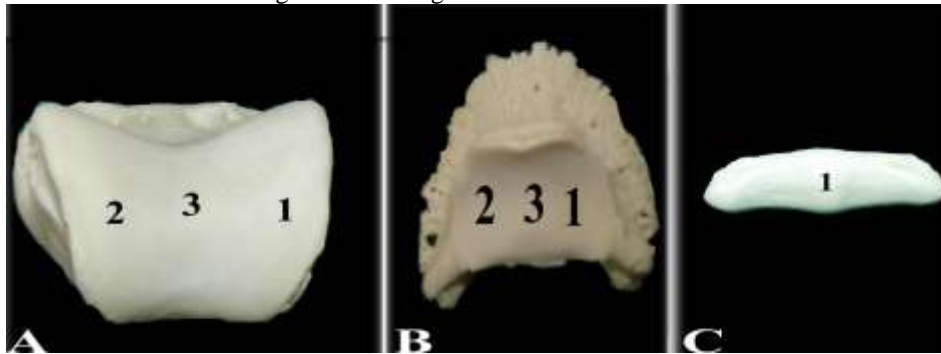


**Figure (8)** photograph of the articular surfaces of the coffin joint of the donkey. A= distal extremity of the 2<sup>nd</sup> phalanx. 1= medial condyle. 2= lateral condyle. 3= sagittal groove. B=3<sup>rd</sup> phalanx. 1= medial articular surface. 2= lateral articular surface. 3=sagittal ridge. C= distal sesamoid bone. 1= vertical ridge.

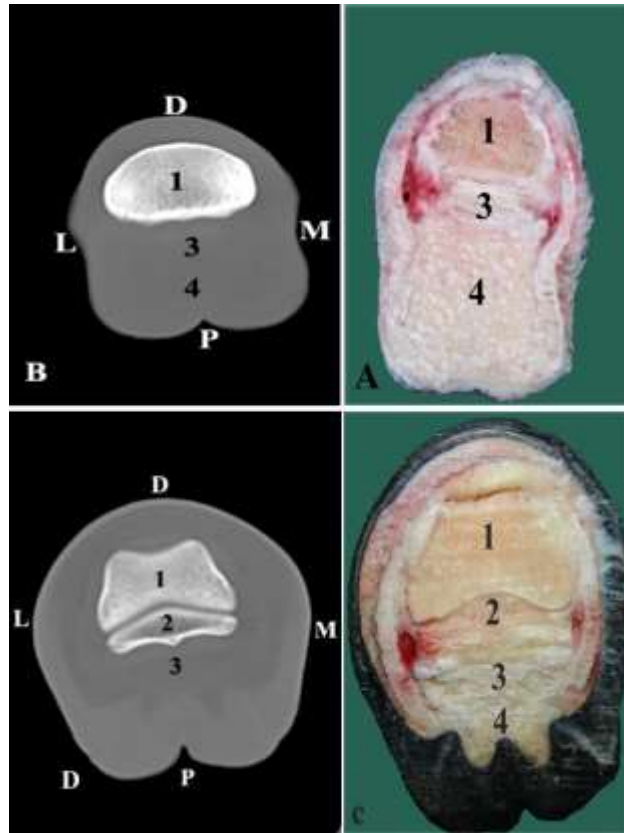


**Figure (9)** photograph of transverse anatomic section (A) and transverse CT views (B) of normal coffin joint of donkey sequentially displayed from proximal to distal. 1= 3<sup>rd</sup> phalanx. 2= distal sesamoid bone. 3= DDFT. 4= digital cushion.



**Figure (10)** photograph of the x-ray film of the fetlock, pastern and coffin joints. 1= 1<sup>st</sup> phalanx. 2= 2<sup>nd</sup> phalanx. 3= 3<sup>rd</sup> phalanx. 4= proximal sesamoid bone. 5=MCI. 6=fetlock joint. 7= pastern joint. 8=coffin joint.